Desalination and Water Treatment
www.deswater.com

doi: 10.5004/dwt.2023.29803

304 (2023) 238–246
August

Remove safranin dye from the aqueous solution using ZnO stabilized on zeolite in the presence of ultraviolet light

Dariush Naghipour[a], Kamran Taghavi[a], Davar Hasanzadeh[a], Seyed Davoud Ashrafi[a,b], Mehrdad Moslemzadeh[a,b,*]

[a]*Department of Environmental Health, School of Health, Guilan University of Medical Sciences, Rasht, Iran, emails: mehrdadmoslemzadh@gmail.com (M. Moslemzadeh), dr.naghipour@gmail.com (D. Naghipour), kam2000ir@yahoo.com (K. Taghavi), d.hasanzadeh69@gmail.com (D. Hasanzadeh), d_ashrafi@gums.ac.ir (S.D. Ashrafi)*
[b]*Research Center of Health and Environment, Guilan University of Medical Sciences, Rasht, Iran*

Received 5 February 2023; Accepted 19 July 2023

ABSTRACT

Dye is one of the most important environmental pollutants which threats human and environmental health. Due to the solubility and high stability of dye in water, incremental attention has been paid to their destruction and removal from industrial effluents. In this study, the efficacy of ZnO nanoparticles coated on natural zeolite (Zeo) as photocatalyst was evaluated to destroy the safranin dye in water solution under UV light. In order to determine the optimal conditions, the effect of dye concentration and solution pH were investigated. Field-emission scanning electron microscopy images show that ZnO is well situated on the Zeo surface and Fourier-transform infrared spectroscopy analysis confirmed the presence of Fe-ZSM5 Zeo and ZnO anatase phase in the synthesized photocatalyst. Optimal values of pH and the dye concentration for dye removal by synthesized UV/ZnO-Zeo photocatalyst were 9 and 100 mg/L, respectively. The maximum safranin dye removal (100%) in optimal conditions under UV light was obtained after 105 min. Also, the maximum adsorption capacity ZnO-Zeo catalyst for safranin was 26.35 mg/g. The removal efficiency reduced from 93% at run first to 32.15% at run fifth. In general, the results showed that the UV/ZnO-Zeo process can be used as an effective and efficient method in removing the safranin from aqueous environments.

Keywords: ZnO; Zeolite; Safranin dye; UV light

1. Introduction

With the increasing population and the expansion of industries and factories, water consumption and wastewater generation are increased. Dye is the most important pollutant released by effluent of the textile industries and other industrial processes [1]. Dyes are organic aromatic compounds that are absorbed in a wavelength of 350–750 nm. Nowadays, dyes are classified into acidic, basic, direct, vat, dispersed, azo, and reactive dyes depending on how they are used in the dyeing process [2]. The textile industries are among the most important consumers of synthetic dyes and chemicals [3]. The entry of industrial wastewater containing pigments into the water environment reduces water quality and cause toxic effects, carcinogenicity and mutations, and irreparable damage to the environment. Also, the entry of colorful effluents into the receiving water prevents the transfer of sunlight to the aquatic environment and reduces photosynthesis, as well as the disruption of biological processes [4].

One of the most widely used dyes is safranin, which is used in the textile industries, medical and laboratory sciences. Various methods such as adsorption processes, oxidation–reduction, ozonation, biological methods, coagulation, and flocculation are used to treat wastewater containing

* Corresponding author.

paint [5]. Common processes for the treatment of these effluents, such as adsorption or coagulation, are not effective enough because they lead to incomplete destruction of pollutants. Also, the use of adsorbents is usually expensive and costly. Oxidation–reduction also requires the addition of additional chemicals to the wastewater, which results in secondary contamination [6,7]. Advanced oxidation processes are one of the most effective treatment methods, which is based on the ability to destroy hazardous organic compounds. This process removes many contaminants that cannot be removed by conventional treatment processes such as coagulation, flocculation, and biological treatment methods [8]. These processes are based on the production of free hydroxyl radicals with high-oxidation power, which converts organic chemical pollutants into minerals and is most effective in oxidizing resistant organic compounds [9]. When the energy of a photon is equal to or greater than the energy gap of semi-conductor, the result is the excitation of an electron from the valance band to the conduction band, which leads to the production of a hole in the valance band due to the excitation of the electron. Excited electrons can directly or indirectly produce hydroxyl radicals, which convert by organic matter into minerals [10].

The photocatalytic mechanism of the semiconductor can be divided into five main stages: first, the transfer of reactants in the liquid phase to the surface, second, the adsorption of the reactants, third, the reaction in the adsorbed phase, fourth, the adsorption of products, and fifth, the removal of products from interphase region [11]. In advanced oxidation with photocatalytic technology, a semiconductor such as ZnO is used to optically excite the electrons of the valance band to the conduction band under the influence of UV radiation. These excited electrons transferred to the conduction bands, along with the positive pores created in the catalyst valance band, are used to produce hydroxyl radical [12]. Hydroxyl radicals are produced in aqueous media using H_2O_2, UV/H_2O_2, UV/TiO_2, UV/ZnO and other methods [13].

The ZnO is due to its direct bandgap energy, bonding energy of 60 megaelectron V, its stability against optical and chemical corrosion, its non-toxicity, insolubility, its ability to decompose toxic organic compounds, its ability to absorb a wide range of electromagnetic waves, and its photocatalytic ability for oxidation of a wide range organic compounds in presence of radiation and is used as an important semiconductor material [14]. Despite the good photocatalytic performance, low adsorption is the limitation of the use of these semiconductors. To address this limitation, many attempts have been made to improve photocatalytic efficiency by using appropriate substrates [15]. Some researchers work on Direct Blue 53 dye using a ZnO catalyst stabilized on activated carbon [16], utilizing TiO_2 and nanoparticles HZSM-5 zeolite to remove reactive dye 2 [17], and the photocatalytic removal of methylene orange using titanium oxide stabilized on activated carbon [18]. Although, activated carbon is widely used as an adsorbent, it has disadvantages such as high cost of production, recycling and regeneration [19]. Due to their unique structure and properties such as high adsorption power, high specific surface area, thermal stability, hydrophilicity, abundance and cheapness, zeolites (Zeo) are more superior and better performance compared to other adsorbents as substrates [20].

In this study, the efficacy of safranin dye removal by the synthesis of ZnO nanoparticles and its stabilization on clinoptilolite Zeo in the presence of UV rays has been investigated. The effective factors studied include the initial amount of ZnO-Zeo oxide nanoparticles, reaction time, pH, initial concentration of safranin, and the effect of the recyclable catalyst.

2. Materials and methods

2.1. Materials

The research was conducted on a laboratory scale. In this study, nitric acid, potassium dichromate, sodium hydroxide, ethanol was produced from Merck, Germany. The natural Zeo of clinoptilolite (mines of Semnan Province) was prepared from the Tejarat Novin Company. A 12-W UV lamp (Philips Co., Germany) was also used as a UV source. The interior is made of a 1 L glass reactor with a UV lamp inside a quartz cylinder. The outer part of the reactor is covered with a larger reactor with a volume of 8 L of water to provide a temperature of 25°C. The variables in question were studied. A hole was also made at the top of the reactor to take the sample. To provide the condition for better irradiation of the sample and to avoid the loss of the reflected light, the lamp was placed in the center of the container in the solution. Moreover, the reactor was completely covered with aluminum foil for better sample irradiation and protection against the carcinogenic effects of UV rays. During the test, the contents of the reactor are shaken by a magnet. On the other hand, hydrochloric acid and sodium hydroxide were used to regulate the pH.

2.2. Zeolite preparation

The natural Zeo of clinoptilolite was crushed by a mortar after preparation in the laboratory and was meshed with sieve No. 30. To remove fine particles and salts, the Zeo samples were washed three times with distilled water, then dried in an oven at 100°C for 24 h to remove moisture from its internal cavities [20].

2.3. Synthesis of ZnO nanoparticles

The hydrothermal method was used to synthesize ZnO nanoparticles. For this purpose, 6 g of zinc chloride was poured into 100 mL of double-distilled water and stirred for 2 h by a magnet. The sodium hydroxide solution was then instilled in it. At the same time, the pH of the solution was controlled. Addition of the sodium hydroxide solution was continued until the pH reached 11. It was then stirred for 7 h by the shaker. Finally, the white precipitate was washed several times with distilled water and dried at room temperature. It was then calcined at 300°C in a furnace [21].

2.4. Preparation of ZnO-Zeo composite

The preparation of the composite continued according to the above method. The zinc chloride was added to double distilled water and then, 10 g of Zeo was added to the above solution and until the pH reached 12, sodium hydroxide was added drop by drop. The resulting sediment was then extracted and calcined as shown above [1,21].

2.5. Photocatalytic degradation of dye

To perform the experiments, the safranin stock solution was first diluted by dissolving 1 g/L of water twice. Factors investigated in this study included the initial concentration of dye (50, 100, 150, and 200 mg/L), the amount of catalyst (0.1, 0.25, 0.5, 0.75, and 1 g/L), pH (3, 5, 7, and 9) and the effect of recycled catalyst. Given that there are two important processes for photocatalytic removal is reduction and adsorption, for starting the photocatalytic tests, nanocomposite and safranin dye were placed in the dark for 15 min to reach equilibrium. Then, the UV lamp was light and the contents of the reactor were stirred by the mixer. The magnetism was disturbed. The experiments were performed by keeping constant of the three variables and changing one variable. For example, at pH of 5 and the composite dosage of 1 g/L, different concentrations of safranin dye were added to the reactor and sampled at different times. The removal percentage of safranin was calculated using Eq. (1):

$$\text{Effeciency}(\%) = \frac{C_0 - C_e}{C_0} \times 100 \quad (1)$$

where C_0 is the initial concentration of safranin in the solution (mg/L) and C_e is the equilibrium concentration (mg/L). The equilibrium adsorption capacity was determined using Eq. (2):

$$\text{Effeciency}(\%) = \frac{(C_0 - C_e)V}{M} \quad (2)$$

where C_0 is the initial concentration of safranin in the solution (mg/L), C_e is the equilibrium concentration (mg/L), q_e is the equilibrium adsorption capacity (mg/L), m is the mass of the adsorbent (g), and V is the volume of solution (L).

In final, data analysis was performed using Excel 2019 software. The residual concentration of safranin, after centrifugation, was measured by a spectrophotometer (DR5000) at a wavelength of 518 nm [22].

2.6. Determination of pH_{ZPC}

To determine the pH of the zero point of the nanoparticle, 0.5 g of the catalyst was poured into 250 mL Erlenmeyer flasks and, using the solutions of caustic soda and acid chloride, the pH of solutions was adjusted at 2, 3, 4, 5, 6, 7, 8, 9, 10, 11, and 12 and mixed with the shaker at rpm 150 for 48 h. After that period, the final pH values were read and the initial and final pH was plotted against each other in a diagram. The intersection point of the graphs was determined as the pH of the zero point of the catalyst [23].

3. Results and discussion

3.1. Structural characterization of adsorbent

3.1.1. X-ray fluorescence spectroscopy study

To analysis chemicals of the catalysts, X-ray fluorescence spectroscopy (XRF) was used using a Shimadzu XRF-1800 (Made in Japan). The results of XRF analysis (Table 1) confirm the presence of silica and alumina as the main components along with a small amount of sodium, magnesium, potassium, iron, and titanium dioxide as impurities in the composition of the natural Zeo. The molar ratio of the silicon to aluminum is 2, but mostly due to the substitution of elements such as magnesium and iron in the Zeo structure with aluminum, or due to the presence of quartz, this ratio is more than 2, and the results of X-ray diffraction (XRD) confirm the presence of quartz. CaO and Na_2O levels indicate the presence of calcite and sodium between the Zeo layers. On the other hand, the results show that most of the aluminum is in the form of bentonite, so it is expected that the adsorbed species of pollutants are mainly removed by SiO_2 or Al_2O_3 [24].

3.1.2. XRD study

XRD analysis was used to evaluate the structural properties and identify the formed phases. For this analysis, the Inel Diffractometer EQUINOX 3000 device (made in the United States) was used in the range of 2θ between 10° and 80°. The crystalline structure of the ZnO nanoparticles synthesized by the XRD device is shown in Fig. 1a. According to Standard No. JCPDS = 36-1451, clear crystalline peaks of ZnO nanoparticles can be seen at angles 2θ: 37°, 40°, 42°, 55°, 66°, 74°, and 78° indicating the hexagonal structure of nanoparticles [25,26]. According to a study by Benhebal et al. [23], sharp peaks on the graph indicate the good crystallization of ZnO nanoparticles. There are a few other weak peaks with lower intensities at angles 2θ: 59°, 47°, and 32°, which according to the standard JCPDS = 0587-04 indicates the presence of KCl. Also, the peak at 2θ: 63°, 53°, 36°, and 31° indicates the presence of NaCl. Yamamoto et al. [27] reported slight amounts of sulfur impurities in ZnO nanoparticle crystals produced by the chemical method. Another study identified impurities such as copper, cadmium, lead, and magnesium in very small amounts in catalyst used in their study [28]. A researcher reported NaCl peaks in the XRD test in iron nanoparticles synthesized from plant extracts [29]. The XRD pattern recorded for natural Zeo adsorbent presented in Fig. 1b also shows that there are some non-clay impurities in the bentonite adsorbent structure, including

Table 1
Results of X-ray fluorescence spectroscopy analysis for the natural Zeo

Elements	Quantity (%)
SiO_2	42.081
Al_2O_3	10.247
Fe_2O_3	6.119
Na_2O	0.381
MgO	5.182
K_2O	2.661
TiO_2	0.557
MnO	0.138
P_2O_5	0.128
LOI	20.1
CaO	12.352

quartz (Q), calcite (C) and feldspar (F). On the other hand, the formation of sharp and elongated peaks, especially in the 2θ equal to 24.3° and 27°, which are related to quartz, is a proof of the high crystallinity of the adsorbent [22,30].

3.1.3. Field-emission scanning electron microscopy study

The surface morphology of synthesized samples was analyzed by field-emission scanning electron microscopy (FE-SEM) analysis using the Hitachi S-4160 device made in Japan. FE-SEM image of Zeo-ZnO before Fig. 2a and after b process. According to the FE-SEM analysis image before process, a uniform appearance with small lumps and swellings can be morphologically attributed to natural bentonite (Fig. 2a). As a result of stabilization of the ZnO on the Zeo, as can be seen in the relevant figure, the Zeo surface is significantly covered with ZnO nanoparticles. ZnO nanoparticles appear to have non-uniform shapes with large granules (20–30 nm) and these particles are evenly and uniformly placed on the surface of the Zeo. Recently a researcher studied on the synthesized ZnO nanoparticles and reported a porous and uneven surface for this catalyst [31]. Fig. 2b also shows the FE-SEM image for Zeo-ZnO after process. As shown, the absorbent sites were covered by methylene blue dye molecules.

3.2. Effect of variable parameters on the removal efficiency of the photocatalytic process

3.2.1. Effect of UV radiation, zeolite, ZnO alone in photocatalytic removal

To investigate the effect of different processes in the photocatalytic reduction of safranin dye, the efficacy of Zeo, ZnO, UV alone, and UV/ZnO-Zeo in reducing the safranin dye was examined separately under optimal conditions (pH of 9 and composite value of 0.75 g/L), and the results shown in Fig. 3. As a result, the safranin removal efficiencies of ZnO alone, Zeo, UV alone were 54.66%, 59.85%, and 60.62% by adsorption at a reaction time of 120 min. As can be seen, the efficiency of the UV/ZnO-Zeo process to reduce the safranin was about 87.92%, which was more effective for reducing the safranin compared to other processes. In situations, where UV light was studied alone, the efficiency of dye removal was very low. This suggests that the production of hydroxyl radicals, which require the formation of catalysts,

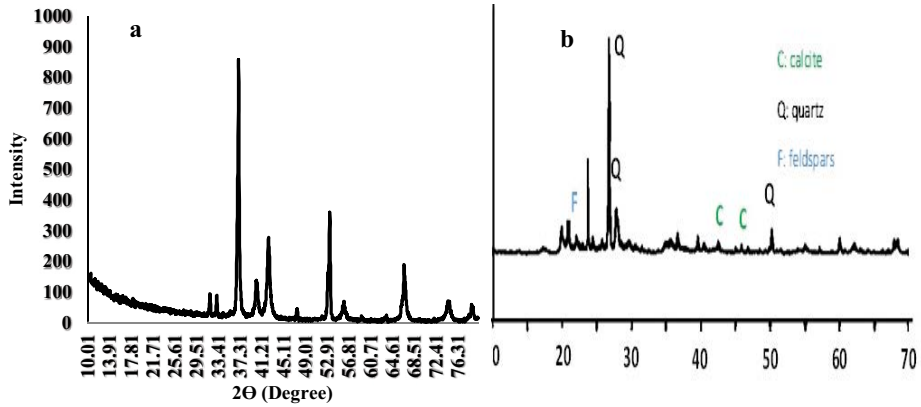

Fig. 1. X-ray diffraction pattern related to synthesized ZnO nanoparticles (a), and Zeo (b).

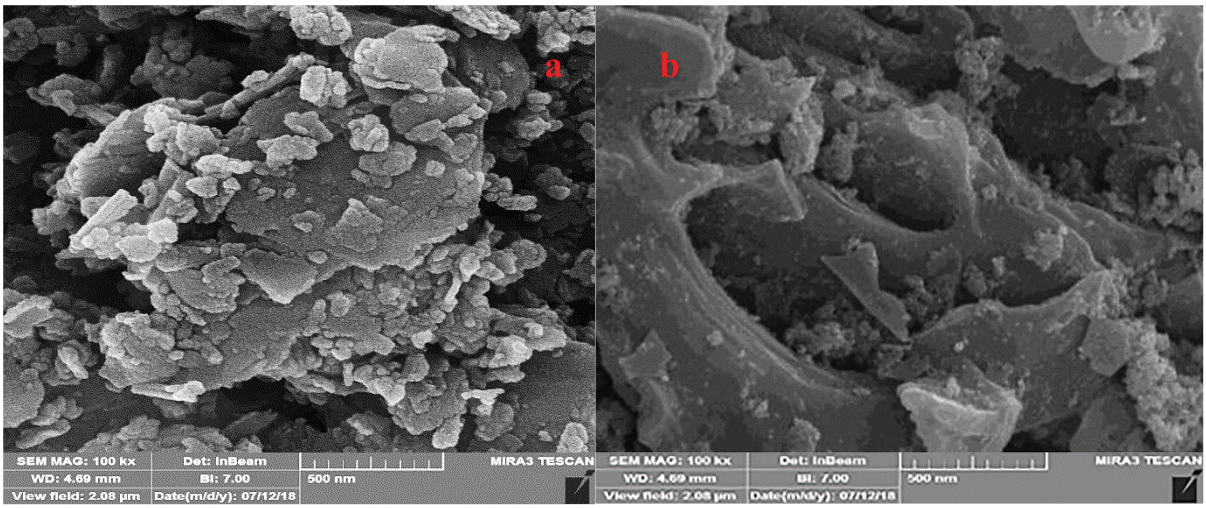

Fig. 2. Field-emission scanning electron microscopy image of Zeo-ZnO before (a) and after (b) process.

plays a major role in initiating the degradation of safranin. It also proves that in the presence of catalysts and UV rays together, electron–hole pairs can be produced, which results in the formation of oxidizing agents to degrade organic contaminants [1,32]. The study conducted on the removal of acid red dye by the titanium oxide-Zeo catalyst in the presence of UV light illuminated that the efficiency of each material alone is less effective than their combination and the highest efficiency of oxidation is related to the TiO_2-Zeo/UV (92.8%), which is consistent with the research results [1].

3.2.2. Effect of pH

The effect of the initial pH of the solution on the efficiency of the process was investigated by changing the initial pH of the solution (3, 5, 7 and 9) under constant conditions, that is, initial safranin concentration of l30 mg/L and constant composite dosage of 0.5 g at different times. Fig. 4a shows the results of the effect of pH on process efficiency. As can be seen, the efficiency of the process increases with increasing pH. As the pH increases from 3 to 9, the removal efficiency increases from 57.28% to 94.72%, respectively.

The cause of this phenomenon is related to the safranin dye structure and the catalyst structure, as well as the pH_{pzc}. With increasing pH, due to increasing the hydroxyl ions level and changing the surface charge of adsorbent, the ionization level of the pollutant increases. In this study, the pH_{zpc} catalyst was obtained to be 7.6; this indicates that at pH values below 7, the catalyst level has a positive charge, and at pH values above 7.16, the catalyst surface has a negative charge. On the other hand, the cationic dye of safranin is ionized due to its cationic structure in the solution, and this leads that its molecules become cationic. For these reasons, by increasing the pH, the surface charge of the catalyst becomes negative and a strong attraction force is created between the catalyst surface and the dye molecules, and this maximum electrostatic attraction causes more adsorption of

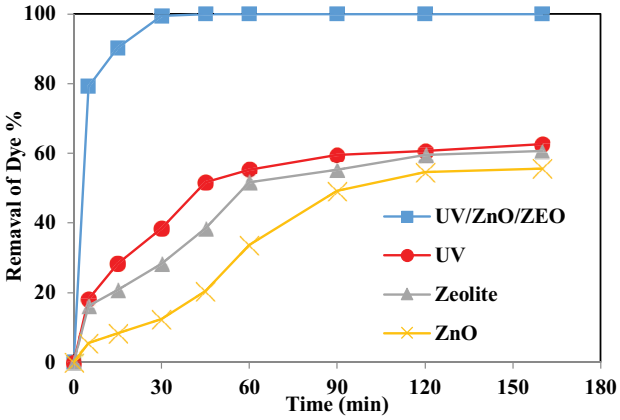

Fig. 3. Effect of UV lamp, zeolite, and ZnO alone in photocatalytic removal (catalyst dosage = 0.75 g/L, pH = 9).

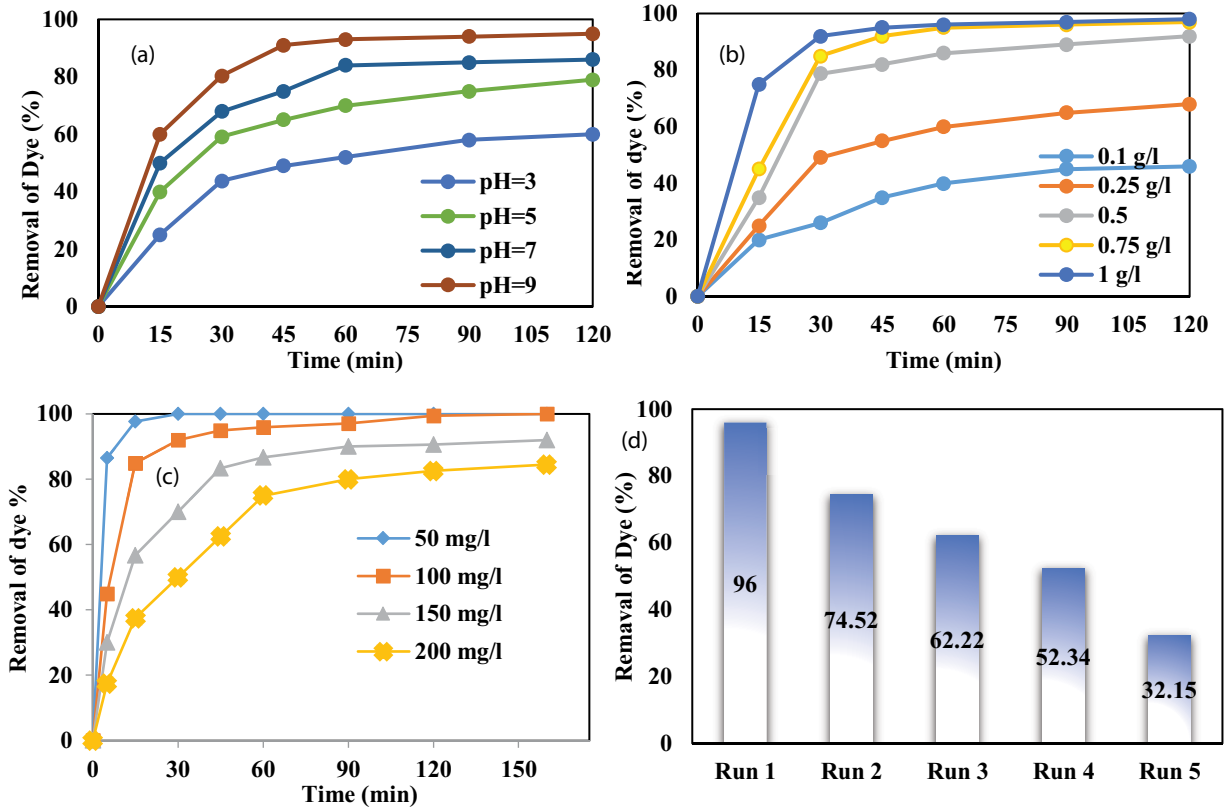

Fig. 4. Effect of variable parameters on the removal of safranin dye: (a) effect of initial pHs (catalyst dosage = 0.75 g/L, safranin c = 30 mg/L), (b) effect of initial dosage (safranin concentration = 100 mg/L, pH = 9), (c) effect of initial concentration of safranin dye (catalyst dosage = 0.75 g/L, pH = 9), and (d) reusability of catalyst (catalyst dosage = 0.75 g/L, dye concentration = 50 mg/L, pH = 9).

contaminants on the catalyst surface and thus further degradation [33,34]. In the study on the photocatalytic removal of safranin dye by titanium oxide, it was reported that with increasing the pH from 2 to 12 increased the efficiency of removal [35]. Another study worked on the removal of safranin dye with titanium-silver oxide, showed increasing the pH from 3 to 12 has significantly led to developing the safranin dye removal efficiency significantly [36].

3.2.3. Effect of the dosage of composite

The effect of the dosage of composite on the removal efficiency of the photocatalytic process to observe the effect of the initial dosage of composite, different values (0.1, 0.25, 0.5, 0.75 and 1 g/L) were investigated under constant conditions including pH of 9 and the initial safranin concentration of 100 mg/L. Fig. 4b displays the results of the effect of the initial composite dosage on the photocatalytic removal process of safranin. As can be seen, increasing the amount of composite from 0.1 to 1 g/L increases the percentage of photocatalytic removal from 40% to 96.27%. Determining the amount of adsorbent due to economic considerations is one of the most important issues in adsorption systems. As experimental, the maximum adsorption capacity ZnO-Zeo catalyst for safranin was 26.35 mg/g. By increasing the catalyst dosage, the safranin removal efficiency increases due to the fact that more surface is provided for dye adsorption and the contact between pollutant and substrate surface [37]. As can be seen from the results, increasing the amount of ZnO-Zeo catalyst increases the efficiency of safranin dye removal. In a past study, it has shown that increasing the concentration of the ZnO catalyst increases the rate of photocatalytic degradation due to the increase in radical hydroxyl production [38,39]. As shown in Fig. 4b, increasing the catalyst dosage to values higher than the optimal dosage does not have a significant effect on removal efficiency; this can be due to the maximum absorption of photons in the reactor and the reduction of active sites available and prevent the formation of electron-cavity pairs, which consistent with results of similar studies [40].

3.2.4. Effect of initial concentration of safranin dye on photocatalytic removal

To observe the effect of the initial concentration of safranin dye, different values (50, 100, 150, and 200 mg/L) were prepared from stock solution and tested under constant conditions (pH = 9 and composite value of 0.75 g/L) at different times. Fig. 4c shows the results of the effect of the initial concentration of safranin dye on the removal efficiency of the photocatalytic process. As can be seen, the removal efficiency decreases with increasing the initial safranin dye concentration, so that when the initial concentration of safranin dye increases from 50 to 200, the removal efficiency decreases from 100% to 84%. At higher concentrations of inlet contaminants, large amounts of contaminants are absorbed on the ZnO catalyst, which prevents photons from reaching the catalyst surface and thus reduces the production of hydroxide radicals, thus reducing the removal efficiency [23,41]. Also, in another study conducted on the photocatalytic removal of safranin dye with titanium oxide, it was found that by increasing the initial amount of safranin dye, the removal efficiency decreased, which is consistent with the present study [35]. Additionally, study on the dye removal by photocatalytic process showed the dye removal efficiency depends on the amount of hydroxyl radical produced. And the study expressed that by increasing the dye concentration, the dye molecules absorb the photon emitted from the UV lamp and prevent reaching them the catalyst leads to less production of hydroxyl radical, which is consistent with research results [42].

3.2.5. Reusability of catalyst

To observe the efficiency of the recycled catalyst in the photocatalytic removal of safranin dye, the catalyst was first washed and regenerated with NaOH solution, it was used to remove the removal percentage under constant conditions (pH of 9, the composite dosage of 0.75 g/L, and initial safranin concentration of 50 mg/L). Fig. 4d shows the efficiency of removing safranin dye using recycled catalyst. As can be seen, the removal efficiency reduced from 93% at run first to 32.15% at run fifth. This reduction in the removal efficiency may be because of aging pollution in the photocatalyst pores.

3.2.6. Kinetic studies of dye removal reaction

In the present study, the pseudo-first-order and pseudo-second-order models were used. The pseudo-first-order and pseudo-second-order models are listed, respectively. The linear form of the pseudo-first-order model is as follows [43]:

$$\text{Pseudo-first-order equation: } \ln\left(\frac{C}{C_0}\right) = -K_1 t \tag{3}$$

where C_t (mg/L) means the residual concentration of safranin dye at time t, C_0 (mg/L) means the initial concentration of safranin dye, and K_1 (min^{-1}) indicates a constant rate of pseudo-first-order equation.

Linear form of the pseudo-second-order equation is as follows [43]:

$$\text{Pseudo-second-order equation: } \frac{1}{C} - \frac{1}{C_0} = K_2 t \tag{4}$$

where K_2 represents the constant degradation rate.

The kinetic parameters of safranin dye removal in optimal conditions are given, in which pH was 9 and composite dosage was considered 0.75 g/L.

Table 2
Kinetic parameters of safranin dye removal

C_0 (mg/L)	First-order		Second-order	
	K_1 (min^{-1})	R^2	K_2 (L/mg·min)	R^2
50	0.234	0.945	0.056	0.966
100	0.035	0.880	0.010	0.718
150	0.015	0.801	0.0005	0.947
200	0.011	0.882	0.0002	0.964

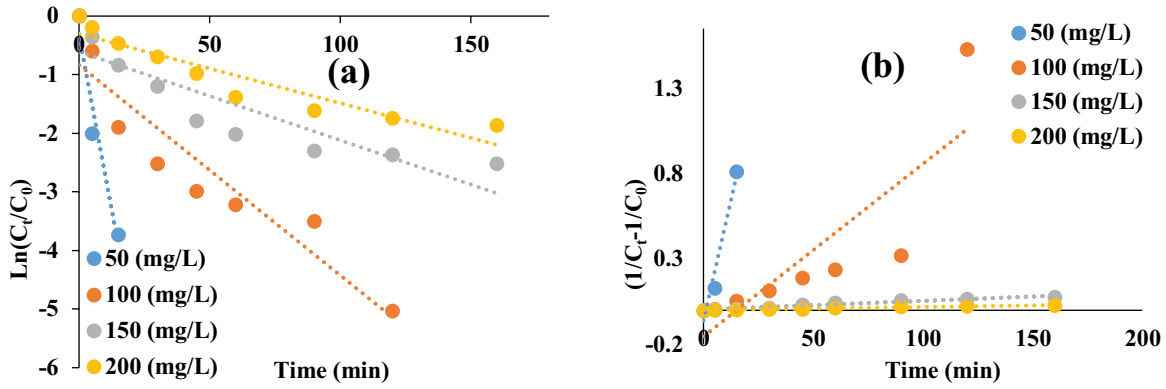

Fig. 5. Results of the first-order quasi-synthetic (a) and second-order (b) quasi-synthetic color of safranin (catalyst dosage = 0.75 g/L, pH = 9).

Table 3
Comparison of maximum adsorption capacity (q_m) of different adsorbents

Catalysts	Dyes	Maximum adsorption capacity (mg/g)	References
Magnetic mesoporous clay	Safranin	18.48	[44]
Poly(vinylidene fluoride) nanofibers	Safranin	25.896	[45]
Corncob activated carbon	Safranin	35.698	[46]
UV/ZnO-Zeo	Safranin	26.35	Present study

Table 2 shows the kinetic parameters of safranin dye degradation. According to Fig. 5 and Table 2 and comparing the correlation coefficients, it can be concluded that the process equilibrium has more obedience from the pseudo-second-order model. Also, the value of q_e calculated in this model is very close to the value of q_e obtained from laboratory data.

3.2.7. Comparison of studies

In Table 3, a comparison of maximum adsorption capacity (q_m) of different catalysts for different dyes is prepared. As shown, ZnO-Zeo catalyst in present study has a promising q_m in comparison of other studies.

4. Conclusion

The results of FE-SEM and XRD analyzes showed the accurate structure of the catalyst and uniform presence of ZnO nanoparticles on the Zeo surface. Increasing the initial concentration of safranin dye significantly reduces the elimination efficiency. The highest the safranin removal efficiency (100%) was obtained for the initial concentration of 50 mg/L at a pH of 9. Also, the maximum adsorption capacity ZnO-Zeo catalyst for safranin was 26.35 mg/g. It should be noted that the UV/ZEO-ZnO process showed better efficiency in the removal of dye compared to ZnO nanoparticles and Zeo. Moreover, the catalyst has the reusability with acceptable removal efficiency, which due to the proper performance of this process in the safranin dye removal, can be used as one of the effective methods in wastewater treatment of textile industries and other industries containing high amounts of dye.

Acknowledgments

The authors appreciate the financial supports of Guilan University of Medical Sciences. Additionally, the authors thank deputy of research and technology of the university and also water and wastewater laboratory of the school of health helped in the implementation of this work.

Disclosure statement

No potential conflict of interest was reported by the author(s).

Funding

This article is taken from the Master's thesis of Environmental Health Engineering, Guilan University of Medical Sciences with grant number 95112315 and ethics code IR. GUMS.REC.1398.53.

References

[1] M. Tanzifi, M. Tavakkoli Yaraki, M. Karami, S. Karimi, A. Dehghani Kiadehi, K. Karimipour, S. Wang, Modelling of dye adsorption from aqueous solution on polyaniline/carboxymethyl cellulose/TiO_2 nanocomposites, J. Colloid Interface Sci., 519 (2018) 154–173.
[2] V.K. Gupta, A. Mittal, R. Jain, M. Mathur, S. Sikarwar, Adsorption of Safranin-T from wastewater using waste materials-activated carbon and activated rice husks, J. Colloid Interface Sci., 303 (2006) 80–86.
[3] K. Cruz-González, O. Torres-López, A. García-León, J.L. Guzmán-Mar, L.H. Reyes, A. Hernández-Ramírez, J.M. Peralta-Hernández, Determination of optimum operating parameters for Acid Yellow 36 decolorization by electro-Fenton

process using BDD cathode, Chem. Eng. J., 160 (2010) 199–206.
[4] A. Kundu, A. Mondal, *In-situ* synthesis of self Ti^{3+} doped TiO_2/RGO nanocomposites as efficient photocatalyst to remove organic dyes from wastewater under direct sunlight irradiation, Mater. Res. Express, 6 (2019) 0850d2, doi: 10.1088/2053-1591/ab22e8.
[5] N. Zaghbani, A. Hafiane, M. Dhahbi, Removal of Safranin T from wastewater using micellar enhanced ultrafiltration, Desalination, 222 (2008) 348–356.
[6] M.R. Sohrabi, M. Ghavami, Photocatalytic degradation of Direct Red 23 dye using UV/TiO_2: effect of operational parameters, J. Hazard. Mater., 153 (2008) 1235–1239.
[7] B. Shi, G. Li, D. Wang, C. Feng, H. Tang, Removal of direct dyes by coagulation: the performance of preformed polymeric aluminum species, J. Hazard. Mater., 143 (2007) 567–574.
[8] M. Qamar, M. Saquib, M. Muneer, Photocatalytic degradation of two selected dye derivatives, chromotrope 2B and amido black 10B, in aqueous suspensions of titanium dioxide, Dyes Pigm., 65 (2005) 1–9.
[9] F. Al-Momani, E. Touraud, J.R. Degorce-Dumas, J. Roussy, O. Thomas, Biodegradability enhancement of textile dyes and textile wastewater by VUV photolysis, J. Photochem. Photobiol. A, 153 (2002) 191–197.
[10] C. Ren, B. Yang, M. Wu, J. Xu, Z. Fu, Y. lv, T. Guo, Y. Zhao, C. Zhu, Synthesis of Ag/ZnO nanorods array with enhanced photocatalytic performance, J. Hazard. Mater., 182 (2010) 123–129.
[11] B. Kakavandi, N. Bahari, R. Rezaei Kalantary, E. Dehghani Fard, Enhanced sono-photocatalysis of tetracycline antibiotic using TiO_2 decorated on magnetic activated carbon (MAC@T) coupled with US and UV: a new hybrid system, Ultrason. Sonochem., 55 (2019) 75–85.
[12] T. Alomar, H. Qiblawey, F. Almomani, R.I. Al-Raoush, D.S. Han, N.M. Ahmad, Recent advances on humic acid removal from wastewater using adsorption process, J. Water Process Eng., 53 (2023) 103679, doi: 10.1016/j.jwpe.2023.103679.
[13] H.T. Chang, N.-M. Wu, F. Zhu, A kinetic model for photo-catalytic degradation of organic contaminants in a thin-film TiO_2 catalyst, Water Res., 34 (2000) 407–416.
[14] W. Xie, Y. Li, W. Sun, J. Huang, H. Xie, X. Zhao, Surface modification of ZnO with Ag improves its photocatalytic efficiency and photostability, J. Photochem. Photobiol., A, 216 (2010) 149–155.
[15] G. Bogoeva-Gaceva, A. Bužarovska, B. Dimzoski, Discoloration of synthetic dyeing wastewater using polyaluminium chloride, G.U. J. Sci., 21 (2008) 123–128.
[16] N. Boudechiche, H. Mokaddem, Z. Sadaoui, Biosorption of cationic dye from aqueous solutions onto lignocellulosic biomass (*Luffa cylindrica*): characterization, equilibrium, kinetic and thermodynamic studies, Int. J. Ind. Chem., 7 (2016) 167–180.
[17] Z. Zhu, J. Yu, Combination of microwave discharge electrodeless lamp and a TiO_2/HZSM-5 composite for the photocatalytic degradation of dimethyl sulphide, Environ. Res., 197 (2021) 111082, doi: 10.1016/j.envres.2021.111082.
[18] Y. Li, X. Li, J. Li, J. Yin, Photocatalytic degradation of methyl orange by TiO_2-coated activated carbon and kinetic study, Water Res., 40 (2006) 1119–1126.
[19] S. Wang, Y. Boyjoo, A. Choueib, Z.H. Zhu, Removal of dyes from aqueous solution using fly ash and red mud, Water Res., 39 (2005) 129–138.
[20] G. Lv, Z. Li, W.-T. Jiang, C. Ackley, N. Fenske, N. Demarco, Removal of Cr(VI) from water using Fe(II)-modified natural zeolite, Chem. Eng. Res. Des., 92 (2014) 384–390.
[21] M. Li, G. Li, J. Jiang, Y. Tao, K. Mai, Preparation, antimicrobial, crystallization and mechanical properties of nano-ZnO-supported zeolite filled polypropylene random copolymer composites, Compos. Sci. Technol., 81 (2013) 30–36.
[22] M. Mahdavianpour, S. Ildari, M. Ebrahimi, M. Moslemzadeh, Decolorization and mineralization of methylene blue in aqueous solutions by persulfate/Fe^{2+} process, J. Water Chem. Technol., 42 (2020) 244–251.
[23] H. Benhebal, M. Chaib, T. Salmon, J. Geens, A. Leonard, S.D. Lambert, M. Crine, B. Heinrichs, Photocatalytic degradation of phenol and benzoic acid using zinc oxide powders prepared by the sol–gel process, Alexandria Eng. J., 52 (2013) 517–523.
[24] T.S. Anirudhan, M. Ramachandran, Adsorptive removal of basic dyes from aqueous solutions by surfactant modified bentonite clay (organoclay): kinetic and competitive adsorption isotherm, Process Saf. Environ. Prot., 95 (2015) 215–225.
[25] R. Pandimurugan, S. Thambidurai, Novel seaweed capped ZnO nanoparticles for effective dye photodegradation and antibacterial activity, Adv. Powder Technol., 27 (2016) 1062–1072.
[26] S. Rajaboopathi, S. Thambidurai, Green synthesis of seaweed surfactant based CdO-ZnO nanoparticles for better thermal and photocatalytic activity, Curr. Appl. Phys., 17 (2017) 1622–1638.
[27] O. Yamamoto, J. Sawai, T. Sasamoto, Change in antibacterial characteristics with doping amount of ZnO in MgO–ZnO solid solution, Int. J. Inorg. Mater., 2 (2000) 451–454.
[28] D. Hasanzadeh, S.D. Ashrafi, K. Taghavi, D. Naghipor, Photocatalytic removal of hexavalet chromium from aqueous solution using zinc oxide nanoparticle stabilized on zeolite, J. Health, 11 (2020) 37–50.
[29] M. Leili, M. Fazlzadeh, A. Bhatnagar, Green synthesis of nano-zero-valent iron from nettle and thyme leaf extracts and their application for the removal of cephalexin antibiotic from aqueous solutions, Environ. Technol. (United Kingdom), 39 (2018) 1158–1172.
[30] K. Taghavi, D. Naghipour, A. Mohagheghian, M. Moslemzadeh, Photochemical degradation of 2,4-dichlorophenol in aqueous solutions by Fe^{2+}/peroxydisulfate/UV process, Int. J. Eng., 30 (2017) 15–22.
[31] F. Zhang, X. Chen, F. Wu, Y. Ji, High adsorption capability and selectivity of ZnO nanoparticles for dye removal, Colloids Surf., A, 509 (2016) 474–483.
[32] M.A. Barakat, Adsorption and photodegradation of Procion yellow H-EXL dye in textile wastewater over TiO_2 suspension, J. Hydro-Environ. Res., 5 (2011) 137–142.
[33] A. Saeed, M. Iqbal, S.I. Zafar, Immobilization of *Trichoderma viride* for enhanced methylene blue biosorption: batch and column studies, J. Hazard. Mater., 168 (2009) 406–415.
[34] A. Mills, S. Le Hunte, An overview of semiconductor photocatalysis, J. Photochem. Photobiol. A, 108 (1997) 1–35.
[35] V.K. Gupta, R. Jain, A. Mittal, M. Mathur, S. Sikarwar, Photochemical degradation of the hazardous dye Safranin-T using TiO_2 catalyst, J. Colloid Interface Sci., 309 (2007) 464–469.
[36] M. El-Kemary, Y. Abdel-Moneam, M. Madkour, I. El-Mehasseb, Enhanced photocatalytic degradation of Safranin-O by heterogeneous nanoparticles for environmental applications, J. Lumin., 131 (2011) 570–576.
[37] S. Chakrabarti, B.K. Dutta, Photocatalytic degradation of model textile dyes in wastewater using ZnO as semiconductor catalyst, J. Hazard. Mater., 112 (2004) 269–278.
[38] A.S. Yusuff, K.A. Thompson-Yusuff, O.D. Adeniyi, M.A. Olutoye, Siliceous termite hill supported ZnO-TiO_2 as a solar light responsive photocatalyst: synthesis, characterization and performance in degradation of methylene blue dye, Surf. Interfaces, 34 (2022) 102360, doi: 10.1016/j.surfin.2022.102360.
[39] A.J. Jafari, M. Moslemzadeh, A. Esrafili, R.R. Kalantary, Synthesis of new composite based on TiO_2 immobilized in glass fibers for photo-catalytic degradation of chlorobenzene in aqueous solutions, Environ. Res., 204 (2022) 112018, doi: 10.1016/j.envres.2021.112018.
[40] I.K. Konstantinou, T.A. Albanis, TiO_2-assisted photocatalytic degradation of azo dyes in aqueous solution: kinetic and mechanistic investigations: a review, Appl. Catal., B, 49 (2004) 1–14.
[41] A.J. Jafari, M. Moslemzadeh, Synthesis of Fe-doped TiO_2 for photocatalytic processes under UV-Visible light: effect of preparation methods on crystal size—a systematic review study, Comments Inorg. Chem.: J. Crit. Discuss. Curr. Lit., 40 (2020) 327–346.

[42] J.-M. Lee, M.-S. Kim, B. Hwang, W. Bae, B.-W. Kim, Photodegradation of acid red 114 dissolved using a photo-Fenton process with TiO_2, Dyes Pigm., 56 (2003) 59–67.
[43] N. Khabaz, J. Jaafari, D. Naghipour, K. Taghavi, M. Moslemzadeh, New hybrid process of peroxymonosulfate activation on the $BiPO_4$ to photocatalytic degradation of diclofenac sodium in aqueous solution, Int. J. Environ. Anal. Chem., (2022) 1–14, doi: 10.1080/03067319.2022.2142047.
[44] M. Fayazi, D. Afzali, M.A. Taher, A. Mostafavi, V.K. Gupta, Removal of Safranin dye from aqueous solution using magnetic mesoporous clay: optimization study, J. Mol. Liq., 212 (2015) 675–685.
[45] S. Sharafinia, A. Farrokhnia, E. Ghasemian Lemraski, Optimized safranin adsorption onto poly(vinylidene fluoride)-based nanofiber via response surface methodology, Mater. Chem. Phys., 276 (2022) 125407, doi: 10.1016/j.matchemphys.2021.125407.
[46] S. Preethi, A. Sivasamy, S. Sivanesan, V. Ramamurthi, G. Swaminathan, Removal of safranin basic dye from aqueous solutions by adsorption onto corncob activated carbon, Ind. Eng. Chem. Res., 45 (2006) 7627–7632.